Successful Decontamination of $^{99}TcO_4^-$ in Groundwater at Legacy Nuclear Sites by a Cationic Metal-Organic Framework with Hydrophobic Pockets

Daopeng Sheng,¶[a] Lin Zhu,¶[b] Xing Dai,¶[a] Chao Xu,[c] Peng Li,[d] Carolyn Pearce,[e] Chengliang Xiao,*[a,f] Jing Chen,[c] Ruhong Zhou,[a] Tao Duan,[b] Omar K. Farha, [d] Zhifang Chai,[a] and Shuao Wang*[a]

Abstract: ^{99}Tc contamination at legacy nuclear sites is one of the most serious and yet unsolved environmental issues associated with nuclear power development. Selective remediation of $^{99}TcO_4^-$ in the presence of large excess of NO_3^- and SO_4^{2-} from natural waste systems represents a significant scientific and technical challenge given anions with higher charge density are often preferentially sorbed by traditional anion-exchange materials, which is known as the Hofmeister Bias selectivity. We report here a solution to this challenge based on a stable three-dimensional cationic metal-organic framework material, SCU-102 ($Ni_2(tipm)_3(NO_3)_4$), formed by hydrophobic tetradentate neutral ligands and Ni^{2+} ions. SCU-102 exhibits fast sorption kinetics, large capacity (291 mg/g), high distribution coefficient, and most importantly the record high TcO_4^- uptake selectivity among all anion-exchange materials reported to date. This material can almost quantitatively remove TcO_4^- in the presence of large access of NO_3^- and SO_4^{2-}. The decontamination experiments based on both a simulated low activity waste stream, and contaminated groundwater at the Hanford site confirm that SCU-102 represents the optimal Tc scavenger with the highest clean up efficiency. First principle simulation reveals that the origin of the exceptional selectivity is the recognition of TcO_4^- by the abundant hydrophobic pockets in the structure.

Anionic pollutants are challenging to deal with due to their high environmental mobility in general because the majority of natural minerals are either neutral or negative in their net charge.[1] To efficiently remove anionic pollutants from aqueous systems, cationic framework materials that may exhibit strong targeted host/guest interaction are highly desirable.[2] Over the past decade, the number of known cationic framework materials has grown exponentially.[3] These materials include but are not limited to natural hydrotalcite clays (also known as layered double hydroxides),[4] cationic lanthanide hydroxide,[5] cationic polymeric materials,[6] and cationic metal-organic frameworks (MOFs).[7] For the majority of these materials, the electrostatic interaction dominates the overall host/guest interaction and therefore those anionic guests with higher charge density generally possess a priority to be captured into the cationic framework. This general trend is known as the Hofmeister Bias selectivity and the removal of low-charge anionic pollutants is very challenging.[2b-e] Among these, remediation of $^{99}TcO_4^-$ from contaminated natural water systems is a typical case. In United States, contamination of $^{99}TcO_4^-$ in groundwater at both Hanford and Savannah River sites is a severe issue as a result of both planned and unplanned discharge of liquid nuclear waste to the subsurface, resulting in concentrations at least an order of magnitude higher than the federal drinking water limit of 900 pCi/L.[8] This issue remains unsolved, partially originating from that TcO_4^- has a low charge density while in the contaminated water systems, anions with higher charge densities such as NO_3^- and SO_4^{2-} often coexist in huge excess. In some cases, anions with even higher charge density i.e. PO_4^{3-} and SiO_3^{2-} may also be present.[9] Anion-exchange selectivity is therefore the key parameter to pursue for practical application purposes.

We recently presented two general strategies for building specific types of cationic MOFs to reverse the Hofmeister bias aiming at the selective TcO_4^- remediation. One is the utilization of relatively soft open metal site (e.g. Ag^+) that can selectively coordinate to the anions with low charge density during the anion-exchange process.[7b] This strategy however faces a severe issue of structural transformation induced crystal cracking after the anion-exchange, making the chromatographic extraction application impractical. The other strategy is to build a hydrophobic cationic cavity that can efficiently recognize the low-charge anion through hydrophobic hydrogen bond interaction,[2b-e] where crystal degradation does not necessarily occur during the anion-exchange. However, this strategy was only partially achieved by our recently reported cationic MOF SCU-101 built by the hydrophobic ligand of tetrakis[4-(1-

[a] D. Sheng, Dr. X. Dai, Prof. C. Xiao, Prof. R. Zhou, Prof. Z. Chai, Prof. S. Wang
State Key Laboratory of Radiation Medicine and Protection, School for Radiological and Interdisciplinary Sciences (RAD-X) and Collaborative Innovation Center of Radiation Medicine of Jiangsu Higher Education Institutions, Soochow University
199 Ren'ai Road, Suzhou 215123, China
E-mail: shuaowang@suda.edu.cn
[b] Prof. L. Zhu, Prof. T. Duan
State Key Laboratory of Environmental-Friendly Energy Materials, School of National Defence Science & Technology and National Collaborative Innovation Center for Nuclear Waste and Environmental Safety, Southwest University of Science and Technology
Sichuan Mianyang, 621010, P.R. China.
[c] Prof. C. Xu, Prof. J. Chen
Collaborative Innovation Center of Advanced Nuclear Energy Technology, Institute of Nuclear and New Energy Technology, Tsinghua University
Beijing 100084, China
[d] Dr. P. Li, Prof. O.K. Farha
Department of Chemistry, Northwestern University
2145 Sheridan Road, Evanston, Illinois 60208, USA
[e] Dr. C.I. Pearce
Pacific Northwest National Laboratory, Richland, Washington, 99352, United States
[f] Prof. C. Xiao
College of Chemical and Biological Engineering
Zhejiang University
38 Zheda Road, Hangzhou 310027, China
E-mail: xiaoc@zju.edu.cn

¶ The first three authors contributed equally.

Supporting information for this article is given via a link at the end of the document.

imidazolyl)phenyl]methane (tipm, **Figure 1a**)) and Ni^{2+}.[7a] Unfortunately, the cationic framework of SCU-101 is unexpectedly incorporated by negatively charged and hydrophilic oxalate anions, leading to a decreased positive charge density of the framework and more importantly a sacrificed uptake selectivity towards TcO_4^-. In this work, we report a stable cationic metal-organic framework SCU-102 that can overcome both of these issues and remarkably exhibits the record high TcO_4^- uptake selectivity among all anion-exchange materials reported,[6b, 7a, 7b] leading to the successful decontamination of groundwater at the U.S. Hanford site.

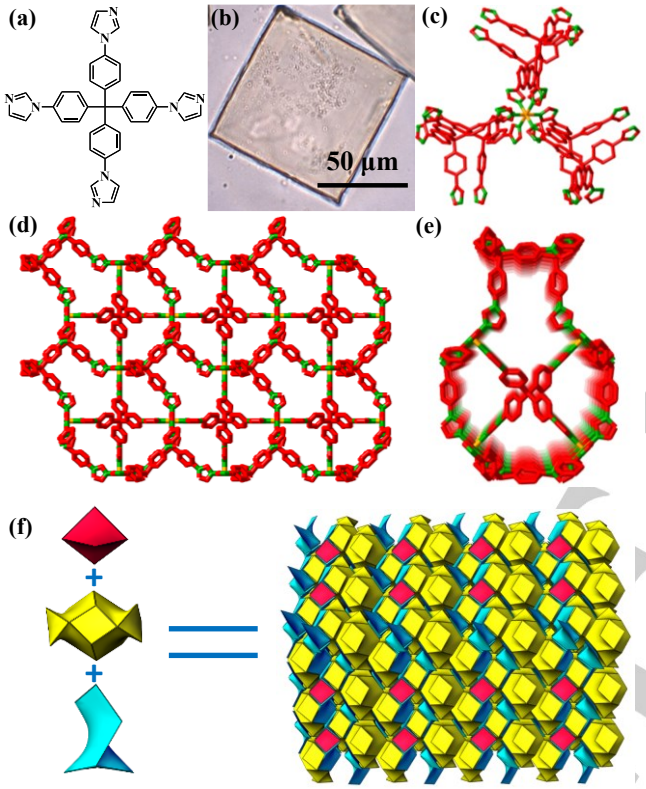

Figure 1. (a) Chemical structure of tipm ligand. (b) Optical image of SCU-102 crystal. (c) Coordination environment of Ni^{2+} with six tipm ligands. (d) Perspective packing structure of SCU-102 viewed along *a* axis. (e) Part of the packing structure of SCU-102. (f) Natural tilings of the structure with three tiles, [4^3] for red tiles, [4.6^2] for cyan tiles, and [4^6.6^6] for yellow tiles. Atom color codes: Ni = orange, N = green, C = light blue.

SCU-102 was prepared by reacting $Ni(NO_3)_2{\cdot}6H_2O$ with tipm ligand in a mixture of water and *N*,*N*-dimethylformamide (DMF) at 100 ºC for 72 h. This reaction condition prevents the decomposition of the ligand and the formation of oxalate groups. The pure cubic crystals with a formula of $Ni_2(tipm)_3(NO_3)_4$ and a size of 80×80×80 μm^3 were obtained (**Figure 1b**). The single crystal X-ray diffraction data shows that SCU-102 crystallizes in a highly symmetric cubic space group of *Pm*-3*n*. The overall structure of SCU-102 can be regarded as a porous three-dimensional cationic nickel-tipm extended framework. Each Ni^{2+} ion is bound by six nitrogen atoms from six different tipm ligands (**Figure 1c**). The average bond length of Ni-N is 2.070 Å. Viewed from all three principle axes, four sets of irregular-shaped one-dimensional channels can be observed (**Figures 1d** and **1e**), also forming a series of pockets mostly surrounded by hydrophobic benzene rings (**Figures S1** and **3a**). The overall structure can be simplied as a 4,6-connected hea topology (**Figure S2a**), which is rarely observed in MOFs.[10] The natural tilings of hea topology are shown in **Figure 1f**. In addition, the cationic framework also contains another set of square channels with a size of 10×10 Å along (111) direction (**Figure S2b**). The overall cationic net charge of the framework is compensated by the disordered nitrate anions, which cannot be identified in the crystal structure, but whose existence was confirmed by ion chromatography analysis and Fourier transform infrared (FT-IR) spectra. Therefore, structural analysis of SCU-102 provides an initial hint that the nitrate anions that initially occupy the hydrophobic pockets can be facilely exchanged out by other types of anions that strongly interact with these pockets.[2b-e]

The stability of SCU-102 in aqueous solution with various pH values and under irradiation was investigated. SCU-102 fully retains its structure in aqueous solution with pH values ranging from 3 to 11 (**Figure S3**). The inductively coupled plasma optical emission spectrometry (ICP-OES) analysis shows that the dissolved Ni^{2+} concentration at equilibrium is 0.23 ppm at pH 7, corresponding to only 0.4 wt% of the total mass of SCU-102, which is notably lower than those of SCU-101 (0.9%) and SBN ([Ag(bipy)]NO_3, bipy= 4,4'-bipyridine) (~50%).[11] After irradiated with 100/200 kGy β and γ irradiations, the PXRD patterns almost duplicate that of the original material (**Figures S4, S5,** and **S6**), suggesting that SCU-102 exhibits decent radiation resistance.

The initial Tc uptake experiment was performed by mixing 20 mg of SCU-102 samples with 20 mL solution containing 28 ppm $^{99}TcO_4^-$. The concentration of TcO_4^- was monitored by both UV-vis absorption spectroscopy and liquid scintillation counting (LSC) measurements. The results show that TcO_4^- was rapidly sorbed by SCU-102, as the characteristic peak of TcO_4^- at 290 nm in the UV-vis spectra almost disappeared at the initial contact time of 10 min (Figure 2a). The sorption equilibrium was reached within 20 min, much shorter than those of other similar cationic MOFs. For example, SLUG-21 and UiO-66-$NH_3^+Cl^-$ require longer than 24 h to reach the equilibrium time.[3a, 12] As clearly seen in **Figures 2b** and **S7**, the sorption kinetics of SCU-102 is faster than those of the-state-of-art anion-exchange resins (Purolite A532E and A530E) that are particularly designed for removing hydrophobic ClO_4^- and TcO_4^-.[2b, 6a,13] The fast sorption rate is mostly attributed to the ordered 1D channels in highly crystalline SCU-102 that allow for efficient transportation of TcO_4^-. The sorption kinetics data can be well fitted by the pseudo-second-order model. The rate constant (k_2) of SCU-102 is 2.48×10^{-2} $g{\cdot}mg^{-1}{\cdot}min^{-1}$, much larger than those of Purolite A532E (4.60×10^{-3} $g{\cdot}mg^{-1}{\cdot}min^{-1}$) and A530E ($6.75\times10^{-3}$ $g{\cdot}mg^{-1}{\cdot}min^{-1}$).

To determine the uptake capacity, a sorption isotherm experiment was carried out. Due to the limited amount of ^{99}Tc that is avaliable, and the radiological operation limits, ReO_4^- was

used as a surrogate for TcO_4^- because they have almost identical charge densities and chemical properties. The identical sorption behaviors of TcO_4^- and ReO_4^- have also been confirmed by our previous work.[7b] In **Figure 2c**, the sorption isotherm curve of SCU-102 towards ReO_4^- is compared with those of NDTB-1 and Mg-Al-LDH (two typical purely inorganic cationic frameworks). All of them can be well fitted to the Langmuir model and the sorption capacity of SCU-102 was calculated to be 291 mg/g. This value is notably higher than those of NDTB-1 and Mg-Al-LDH,[7b, 14] and more importantly higher than the most promising Tc-uptake MOF before this work, SCU-101 (217 mg/g).[7a] This partially originates from the increase of the positive charge density of the cationic framework by elimination of the oxalate group.

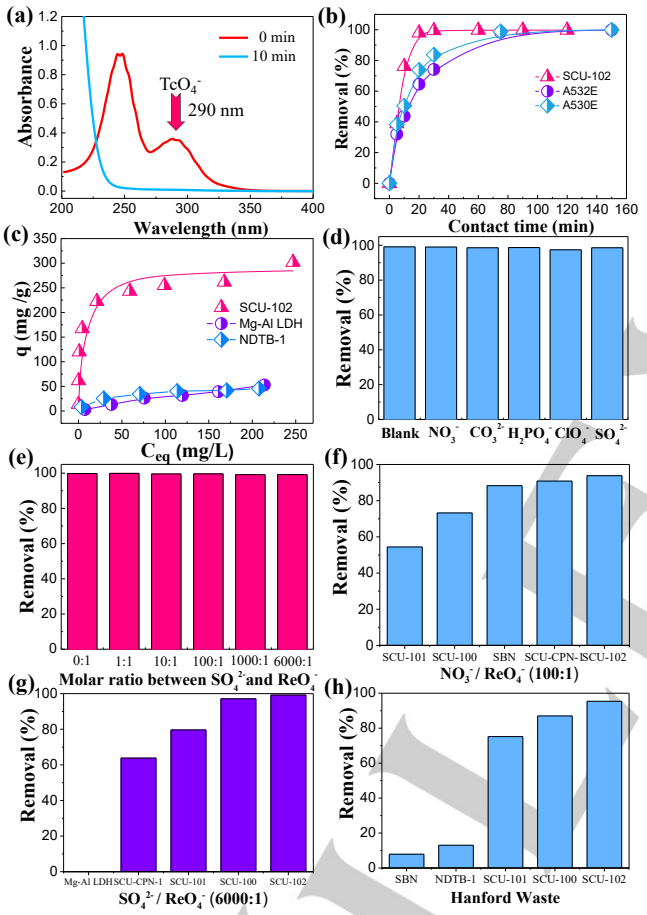

Figure 2. (a) UV-vis absorption spectra of $^{99}TcO_4^-$ as a function of contact time during the anion exchange with SCU-102. (b) Comparison of the sorption kinetic of ReO_4^- by SCU-102, Purolite A532E and A530E resins. (c) Comparison of sorption isotherms of ReO_4^- by SCU-102, Mg-Al-LDH, and NDTB-1. (d) Removal percentage of ReO_4^- by SCU-102 in presence of competitive anions (molar ratio: 1/1). (e) Removal percentage of ReO_4^- by SCU-102 as a function of SO_4^{2-} concentration. (f) Comparison of the selectivity towards ReO_4^- and $^{99}TcO_4^-$ by various sorbents under the condition of large excess of competing anions such as NO_3^- (molar ratio: 100/1) and (g) SO_4^{2-} (molar ratio: 6000/1), and (h) simulated Hanford waste.

We then checked the anion-exchange selectivity of SCU-102 towards TcO_4^-/ReO_4^- in the presence of one equivalent of NO_3^-, CO_3^{2-}, PO_4^{3-}, ClO_4^- or SO_4^{2-}. As shown in **Figure 2d**, those competing anions show negligible effect on TcO_4^-/ReO_4^- removal when their concentrations are low. Interestingly, under such conditions, the removal percentages towards anions with higher charge densities are much lower at 8.7% for PO_4^{3-} and 21.8% for SO_4^{2-}, respectively. Note this represents the reversed case of Hofmeister Bias selectivity. When the amounts of competing anions (NO_3^- and SO_4^{2-}) increase, the sorption properties of SCU-102 towards ReO_4^- are not significantly influenced (**Figures 2e** and **S8**).[7a-c, 15] The removal efficiency of ReO_4^- reaches as high as 98.7% at a molar ratio of 20 (NO_3^-/ReO_4^-). Even at a ratio of 100, SCU-102 can still remove 93.8% of ReO_4^-. For SO_4^{2-}, even if it is in 6000-fold excess, the removal percentage of ReO_4^- is almost quantitative at 99.2%. Impressively, under all tested conditions, the uptake selectivity towards TcO_4^-/ReO_4^- by SCU-102 is notably superior to other reported anion-exchange materials such as SCU-100, SCU-101, SBN, SCU-CPN-1, and Mg-Al LDH material (**Figures 2f** and **2g**). As a useful comparison, the removal efficiencies of ReO_4^- by SCU-101 are 54.4% and 79.6% at the molar ratio of 100 for NO_3^-/ReO_4^- and 6000 for SO_4^-/ReO_4^-, respectively, significantly lower than those of SCU-102.

When tested using a simulated Hanford low activity waste melter recycle stream that contains of NO_3^-, NO_2^-, and Cl^- with ca. 500 times in excess, SCU-102 represents the best scavenger for TcO_4^- with a removal efficiency as high as 95.4%. In contrast, NDTB-1 and SCU-101 can only capture 13% and 75.2% of TcO_4^- under the same condition (**Figure 2h**). This is again consistent with the increase of the hydrophobicity in the open space of SCU-102, compared with that of SCU-101.

The most important experiment showing the real utility is the batch experiment based a simulated Hanford Site groundwater that is contaminated with 1 ppm of ^{99}Tc.[16] This groundwater sample contains SO_4^{2-} CO_3^{2-}, SiO_3^{2-}, and Cl^- at concentrations 4-5 orders of magnitude higher than that of TcO_4^- (**Table S2**), representing a huge decontamination challenge. Very impressively, SCU-102 can quantitatively remove $^{99}TcO_4^-$ from contaminated groundwater sample within one day of contact, and the distribution coefficient (K_d) reaches as high as 5.6×10^5 mL/g. This value is almost one order of magnitude higher than that of SCU-101 (7.17×10^4 mL/g), which shows a clear advantage of SCU-102 when dealing with the real contaminated groundwater.

The SCU-102 material incorporating ReO_4^- was thoroughly characterized by optical microscopy, transmission electron microscope-energy dispersive X-ray spectroscopy (TEM-EDS), Fourier transform infrared (FT-IR) spectroscopy, and powder X-ray diffraction (PXRD) techniques. After the ion-exchange process, SCU-102 retains its cubic morphology (**Figure S9**), a desirable property for chromatographic extraction applications. TEM-EDS element mapping analysis clearly shows that ReO_4^- is uniformly distributed in SCU-102 (**Figure S10**). A new peak at 896 cm^{-1} corresponding to the characteristic vibration of Re-O bond appears in the FT-IR spectrum (**Figure S11**). PXRD patterns verify the structure of SCU-102 remains unchanged after exchanged with ReO_4^-/TcO_4^- (**Figures S6** and **S12**).

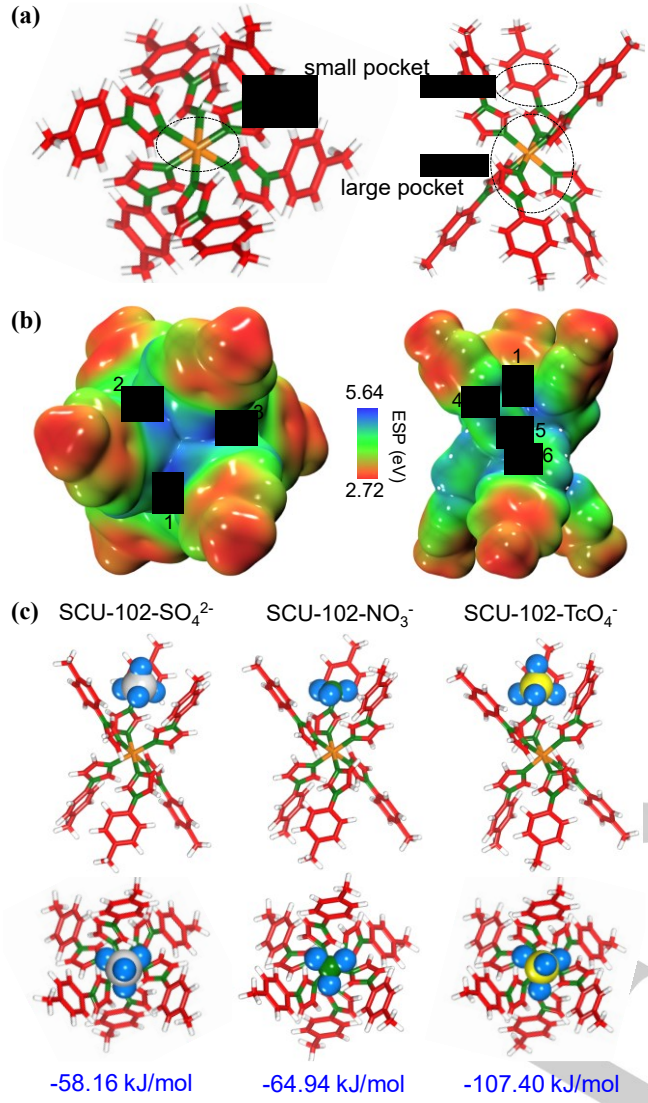

Figure 3. (a) Selected fragment of SCU-102 for DFT calculations, showing two possible recognition sites for anions (small pocket and large pocket), and (b) corresponding electrostatic potentials distribution. (c) Optimized structures of selected fragment of SCU-102 with different anions and corresponding binding energies.

Density function theory (DFT) calculation provides a comprehensive understanding of the anion-exchange process. We selected a typical fragment of SCU-102 as a theoretical model, which consists of one Ni^{2+} cation and six partial ligands. In this model, positive charges on Ni^{2+} are uniformly distributed and transferred to the tipm ligands, especially to the imidazolyl groups, resulting in two possible recognition sites for anions: a small pocket and a large pocket (**Figure 3a**). The electrostatic potential (ESP) distribution of the SCU-102 fragment (**Figure 3b**) reveals there are three maximal values (**1**, **2**, and **3**) on the small pocket, while there are four maximal values on the large pocket (**1**, **4**, **5**, and **6**). The relative ESP values of **1**, **2**, and **3** are all equal to 5.64 eV, which are larger than those of **4** (4.98 eV), **5** (4.90 eV), and **6** (5.17 eV). This suggests that the small pocket may be preferable to accommodate the anionic guests.

Furthermore, the binding energies between SCU-102 and different anions using the small pocket as the model are all higher than those using the large pocket. For example, TcO_4^- is bound in the small pocket of SCU-102 with an energy of -107.40 kJ/mol, while the corresponding binding energy is only -71.25 kJ/mol in the large pocket. We then optimized the structures of the selected fragment of SCU-102 with SO_4^{2-}, NO_3^-, ReO_4^-, and TcO_4^- and calculated their corresponding binding energies using the small pocket as the model (**Figures 3c**). In the optimized structures, three oxygen atoms of the oxo-anions are exactly located in the position of maximal values of ESP. The binding energy of SCU-102-TcO_4^- (-107.40 kJ/mol) is very close to that of SCU-102-ReO_4^- (-113.72 kJ/mol), while both of them are considerably higher than those of SCU-102-SO_4^{2-} (-58.16 kJ/mol) and SCU-102-NO_3^- (-64.94 kJ/mol). This can perfectly explain why SCU-102 exhibits such an exceptional selectivity towards ReO_4^- and TcO_4^-. Considering that the Gibbs energies of hydration of SO_4^{2-} (-1090 kJ/mol) and NO_3^- (-306 kJ/mol) are larger than TcO_4^- (-251 kJ/mol), SCU-102 prefers to bind more hydrophobic anions such as ReO_4^- and TcO_4^- from aqueous solution.

According to the rotation of the ligand, the size of each pocket near the Ni^{2+} cation is actually alterable. The small and large pockets shown in **Figure 3** are the theoretical smallest and largest ones, respectively. Our DFT calculations show that TcO_4^-/ReO_4^- also possess significant larger binding energies (-71.25/-80.71 kJ/mol) than SO_4^{2-} (-42.38 kJ/mol) and NO_3^- (-49.33 kJ/mol), even at the large pocket. Therefore, we conclude that the size of the pocket would not affect the selectivity of SCU-102 towards ReO_4^- and TcO_4^-. The better binding affinity of the small pocket can be mainly attributed to its larger and more concentrated positive ESPs, leading to a favourable steric coordination environment for tetrahedral TcO_4^-/ReO_4^- anions.

In conclusion, a new robust cationic MOF, SCU-102, exhibits high removal efficiency, large sorption capacity, and the highest selectivity towards $^{99}TcO_4^-$. Furthermore, density functional theory calculations clearly reveal the origin of the exceptionally selective TcO_4^- capture, and the possible recognition sites. This work not only reports a promising scavenger that offers a solution to the long-term challenge of ^{99}Tc decontamination from complex natural water systems, but also sheds light on rational design of cationic framework materials for the remediation of other anionic environmental pollutants in the future.

Acknowledgements

This work was supported by the National Natural Science Foundation of China (21825601, 21790374, 11605118, U1732112, 21876124) and the Doctoral Foundation Project of Southwest University of Science and Technology (18zx7148). O.K.F. and P.L. gratefully acknowledge financial support by Northwestern University and the U.S. Department of Energy, National Nuclear Security Administration under Award Number DE-NA0003763. C.I.P. acknowledges support from the Deep Vadose Zone, Applied Field Research Initiative at Pacific Northwest National Laboratory.

Keywords: pertechnetate • metal-organic framework• cationic framework• anion exchange • nuclear waste

[1] J. Icenhower, N. Qafoku, W. Martin, J. M. Zachara, J. **2008,** PNNL-18139.

[2] a) S. R. J. Oliver, *Chem. Soc. Rev.* **2009**, *38*, 1868-1881; b) R. Custelcean, B. A. Moyer, *Eur. J. Inorg. Chem.* **2007**, *2007*, 1321-1340; c) D. Banerjee, D. Kim, M. J. Schweiger, A. A. Kruger, P. K. Thallapally, *Chem. Soc. Rev.* **2016**, *45*, 2724-2739; d) N. Busschaert, C. Caltagirone, W. Van Rossom, P. A. Gale, *Chem. Rev.* **2015**. *115*, 8038–8155; e) Y. Marcus, *J. Chem. Soc. Faraday Trans.* **1991**, *87*, 2995-2999.

[3] a) H. Fei, M. R. Bresler, S. R. J. Oliver, *J. Am. Chem. Soc.* **2011**, *133*, 11110-11113; b) H. Fei, D. L. Rogow, S. R. J. Oliver, *J. Am. Chem. Soc.* **2010**, *132*, 7202-7209; c) H. Fei, L. Paw U, D. L. Rogow, M. R. Bresler, Y. A. Abdollahian, S. R. J. Oliver, *Chem. Mater.* **2010**, *22*, 2027-2032; d) S. Wang, P. Yu, B. A. Purse, M. J. Orta, J. Diwu, W. H. Casey, B. L. Phillips, E. V. Alekseev, W. Depmeier, D. T. Hobbs, T. E. Albrecht-Schmitt, *Adv. Funct. Mater.* **2012**, *22*, 2241-2250; e) A. Karmakar, A. V. Desai, S. K. Ghosh, *Coord. Chem. Rev.* **2016**, *307*, 313-341; f) X. Zhao, C. Mao, K. T. Luong, Q. Lin, Q. G. Zhai, P. Feng, X. Bu, *Angew. Chem. Int. Ed.* **2016**, *55*, 2768-2772.

[4] a) H. W. Olfs, L. O. Torres-Dorante, R. Eckelt, H. Kosslick, *Appl. Clay. Sci.* **2009**, *43*, 459-464; b) Y. Wang, H. Gao, *J. Colloid Interf. Sci.* **2006**, *301*, 19-26.

[5] a) L. Zhu, L. Zhang, J. Li, D. Zhang, L. Chen, D. Sheng, S. Yang, C. Xiao, J. Wang, Z. Chai, T. E. Albrecht-Schmitt, S. Wang, *Environ. Sci. Technol.* **2017**, *51*, 8606-8615; b) L. J. McIntyre, L. K. Jackson, A. M. Fogg, *Chem. Mater.* **2008**, *20*, 335-340; c) H. V. Goulding, S. E. Hulse, W. Clegg, R. W. Harrington, H. Y. Playford, R. I. Walton, A. M. Fogg, *J. Am. Chem. Soc.* **2010**, *132*, 13618-13620.

[6] a) J. Li, L. Zhu, C. Xiao, L. Chen, Z. Chai, S. Wang, *Radiochim. Acta* **2018**, *106*, 581-591; b) D. Banerjee, S. K. Elsaidi, B. Aguila, B. Li, D. Kim, M. J. Schweiger, A. A. Kruger, C. J. Doonan, S. Ma, P. K. Thallapally, *Chem. Eur. J.* **2016**, *22*, 17581-17584; c) Y. Song, Q. Sun, B. Aguila, S. Ma, *Adv. Sci.* **2018**, *0*, 1801410.

[7] a) L. Zhu, D. Sheng, C. Xu, X. Dai, M. A. Silver, J. Li, P. Li, Y. Wang, Y. Wang, L. Chen, C. Xiao, J. Chen, R. Zhou, C. Zhang, O. K. Farha, Z. Chai, T. E. Albrecht-Schmitt, S. Wang, *J. Am. Chem. Soc.* **2017**, *139*, 14873-14876; b) D. Sheng, L. Zhu, C. Xu, C. Xiao, Y. Wang, Y. Wang, L. Chen, J. Diwu, J. Chen, Z. Chai, T. E. Albrecht-Schmitt, S. Wang, *Environ. Sci. Technol.* **2017**, *51*, 3471-3479; c) L. Zhu, C. Xiao, X. Dai, J. Li, D. Gui, D. Sheng, L. Chen, R. Zhou, Z. Chai, T. E. Albrecht-Schmitt, S. Wang, *Environ. Sci. Technol. Lett.* **2017**, *4*, 316-322; d) Y. Li, Z. Yang, Y. Wang, Z. Bai, T. Zheng, X. Dai, S. Liu, D. Gui, W. Liu, M. Chen, L. Chen, J. Diwu, L. Zhu, R. Zhou, Z. Chai, T. E. Albrecht-Schmitt, S. Wang, *Nat. Commun.* **2017**, *8*, 1354; e) L. Ma, J. Yang, B. B. Lu, C. P. Li, J. F. Ma, *Inorg. Chem.* **2018**, *57*, 11746-11752; f) C. P. Li, H. Zhou, S. Wang, J. Chen, Z. L. Wang, M. Du, *Chem. Commun.* **2017**, *53*, 9206-9209; g) X. Li, H. Xu, F. Kong, R. Wang, *Angew. Chem. Int. Ed.* **2013**, *125*, 14014-14018; g) R. J. Drout, K. Otake, A. J. Howarth, T. Islamoglu, L. Zhu, C. Xiao, S. Wang, Farha, O. K. *Chem. Mater.* **2018**, *30*, 1277–1284.

[8] a) C. I. Pearce, J. P. Icenhower, R. M. Asmussen, P. G. Tratnyek, K. M. Rosso, W. W. Lukens, N. P. Qafoku, *ACS Earth Space Chem.* **2018**, *2*, 532-547; b) J. Eagling, P. J. Worsfold, W. H. Blake, M. J. Keith-Roach, *Environ. Sci. Technol.* **2012**, *46*, 11798-11803; c) D. Li, D. I. Kaplan, A. S. Knox, K. P. Crapse, D. P. Diprete, *J. Environ. Radioactiv.* **2014**, *136*, 56-63; d) C. L. Corkhill, J. W. Bridge, X. C. Chen, P. Hillel, S. F. Thornton, M. E. Romero-Gonzalez, S. A. Banwart, N. C. Hyatt, *Environ. Sci. Technol.* **2013**, *47*, 13857-13864.

[9] J. G. Darab, P. A. Smith, *Chem. Mater.* **1996**, *8*, 1004-1021.

[10] M. Li, D. Li, M. O'Keeffe, O. M. Yaghi, *Chem. Rev.* **2014**, *114*, 1343-1370.

[11] a) I. R. Colinas, R. C. Silva, S. R. J. Oliver, *Environ. Sci. Technol.* **2016**, *50*, 1949-1954; b) X. Cui, A. Khlobystov, X. Chen, D. Marsh, A. Blake, W. Lewis, N. Champness, C. Roberts, M. Schröder, Chem. Eur. J. **2009**, *15*, 8861-8873; c) I. R. Colinas, K. K. Inglis, F. Blanc, S. R. J. Oliver, *Dalton Trans.* **2017**, *46*, 5320-5325.

[12] D. Banerjee, W. Xu, Z. Nie, L. E. V. Johnson, C. Coghlan, M. L. Sushko, D. Kim, M. J. Schweiger, A. A. Kruger, C. J. Doonan, P. K. Thallapally, *Inorg. Chem.* **2016**, *55*, 8241-8243.

[13] Y. Zhu, N. Gao, Q. Wang, X. Wei, *Colloids Surf., A* **2015**, *468*, 114-121.

[14] S. Wang, E. V. Alekseev, J. Diwu, W. H. Casey, B. L. Phillips, W. Depmeier, T. E. Albrecht-Schmitt, *Angew. Chem. Int. Ed.* **2010**, *49*, 1057-1060.

[15] J. Li, X. Dai, L. Zhu, C. Xu, D. Zhang, M. A. Silver, P. Li, L. Chen, Y. Li, D. Zuo, H. Zhang, C. Xiao, J. Chen, J. Diwu, O. K. Farha, T. E. Albrecht-Schmitt, Z. Chai, S. Wang, *Nat. Commun.* **2018**, *9*, 3007.

[16] C. I. Pearce, E. A. Cordova, W. L. Garcia, S. A. Saslow, K. J. Cantrell, J. W. Morad, O. Qafoku, J. Matyàš, A. E. Plymale, S. D. Chatterjee, T. G. Levitskaia, M. J. Rigali, J. E. Szecsody, S. Heald, S. Wang, W. L. Queen, R. C. Moore, V. L. Freedman, **2018,** PNNL-SA-138465.

Table of Contents

COMMUNICATION

Cationic Metal-Organic Framework. A robust 3D cationic metal-organic framework material, SCU-102, exhibits fast sorption kinetics, large uptake capacity, high distribution coefficient, and the record high TcO_4^- uptake selectivity, offering a solution to the long-term challenge of ^{99}Tc decontamination from complex natural water systems at the legacy nuclear site.

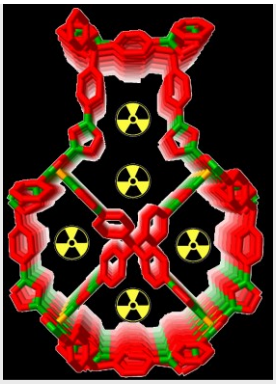

Daopeng Sheng,¶[a] Lin Zhu,¶[b] Xing Dai,¶[a] Chao Xu,[c] Peng Li,[d] Carolyn Pearce,[e] Chengliang Xiao,[a,f] Jing Chen,[c] Ruhong Zhou,[a] Tao Duan,[b] Omar K. Farha,[d] Zhifang Chai,[a] and Shuao Wang*[a]*

Page No. – Page No.

Successful Decontamination of $^{99}TcO_4^-$ in Groundwater at Legacy Nuclear Sites by a Cationic Metal-Organic Framework with Hydrophobic Pockets